

Molecular conduction: paradigms and possibilities

A. W. Ghosh and S. Datta

School of Electrical and Computer Engineering, Purdue University, West Lafayette, IN 47907

We discuss the factors that determine the overall shape and magnitude of the current-voltage (I-V) characteristics of a variety of molecular conductors sandwiched between two metallic contacts. We analyze the individual influences of the contact geometry, the molecular chemistry, the electrostatics of the environment, and charging on molecular conduction. The theoretical predictions depend sensitively on the experimental geometry, as well as on the theoretical model for the molecule and the contacts. Computing molecular I-V characteristics will thus require theoretical understanding on several fronts, in particular, in the scheme for calculating the molecular energy levels, as well as on the position of the contact Fermi energy relative to those levels.

I. MOLECULAR CONDUCTION: WHAT IS THE UNDERLYING PHYSICS?

Recently several researchers have measured charge transport in single or small groups of organic molecules connected to metal contacts [1-9]. In parallel, there have been theoretical attempts at understanding molecular conduction, both at the semi-empirical [3,10-16] and first-principles [17-23] levels. Understanding molecular conduction is challenging, since it involves not just the intrinsic chemistry of the molecule, but extrinsic factors as well, such as the metal-molecule bonding geometry, contact surface microstructure and the electrostatics of the environment. The aim of this article is to discuss the various physical factors that influence molecular current-voltage (I-V) characteristics, and our attempts to model them both qualitatively and quantitatively.

A typical two-terminal molecular I-V looks like Fig. 1, often with a clear conductance gap [1]. How does one understand such an I-V? The first step is to draw an energy-level diagram, as in Fig. 2. An isolated molecule has a discrete set of energy levels, with a highest occupied (HOMO) and a lowest unoccupied molecular orbital (LUMO), separated by a HOMO-LUMO gap (HLG). On connecting the molecule to metallic contacts, two changes happen: (i) the discrete molecular levels broaden into a quasicontinuum density of states (DOS) due to hybridization with the metal wave functions. Often the DOS retains a distinct peak structure, in which case it is still useful to think in terms of broadened molecular energy "levels"; (ii) the difference in work functions between the molecule and the metal causes charge transfer and band alignment between the two materials. The molecule equilibrates with the contact with an overall chemical potential set by the metal Fermi energy E_F , typically lying inside the HLG. Under an applied bias the molecule tries to equilibrate simultaneously with both contacts with bias-separated chemical potentials μ_1, μ_2 , and is thereby driven strongly out of equilibrium. As long as the bias is small and μ_1, μ_2 lie in the HLG, the HOMO levels stay filled and LUMOs are empty and there is no current.

However, when the bias is large enough that either μ_1 or μ_2 crosses a molecular level E_{MOL} , that level is filled (reduced) by one contact and emptied (oxidized) by the other (Fig. 2a) and therefore starts conducting current [24]. For opposite bias, the same level starts conducting when crossed by the other contact chemical potential (Fig. 2b). The net result is that for a spatially symmetric molecule with symmetrically coupled contacts the total conductance gap is given by $4(E_F - E_{MOL})$. Molecular conduction thus depends on both the intrinsic molecular chemistry through E_{MOL} and the contact microstructure through E_F .

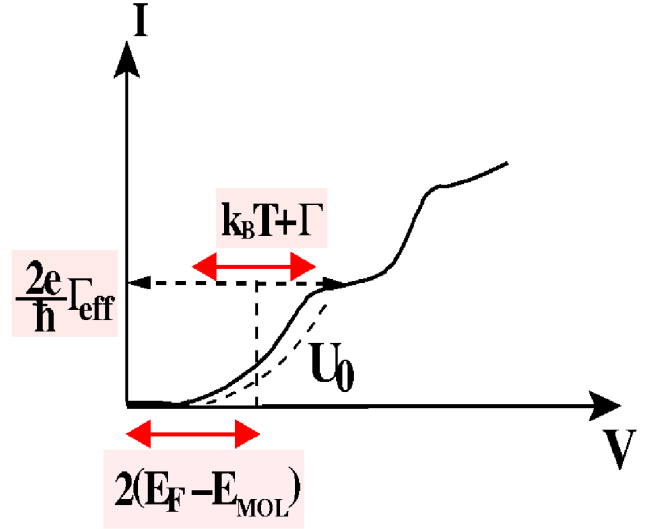


FIG. 1. Generic molecular I-V and parameters controlling it. The current rises when a molecular level E_{MOL} is crossed at a bias $V = 2(E_F - E_{MOL})$, where E_F is the contact Fermi energy. The overall current magnitude is controlled by $\Gamma_{eff} = \Gamma_1 \Gamma_2 / (\Gamma_1 + \Gamma_2)$, Γ_i being the broadenings of the molecular levels by hybridization with the contacts. The current rises over a voltage width set by the thermal broadening $k_B T$ and by $\Gamma = \Gamma_1 + \Gamma_2$. The current is dragged out further by the presence of a Coulomb charging energy U_0 .

The intrinsic chemistry of an isolated molecule can be

handled with sophisticated quantum chemical codes that can be purchased or even downloaded from the Internet. Given an appropriate basis-set (for instance, a minimal STO-3G basis) and an appropriate model for electron-electron interactions (based on first-principles density functional, Hartree-Fock or semi-empirical Huckel methods), such a code starts with an initial guess density matrix to obtain a Fock matrix F (Fig. 3a). It then fills up the corresponding energy eigenstates with a given number N of electrons according to equilibrium statistical mechanics to reevaluate, recalculates F and so on, until self-consistent convergence. Our molecular system differs in two ways: (i) it is open, with a varying, fractional occupancy of electronic levels; (ii) it is trying to equilibrate under bias with two different contact chemical potentials and is therefore driven strongly out of equilibrium. To solve this problem, we modify the above self-consistent scheme, as shown in Fig. 3b. The initial step, solving for the Fock matrix F , is kept unchanged from the usual prescriptions in molecular chemistry. In this step, one can use semi-empirical tight-binding/Huckel-based methods [25], or exploit the sophisticated numerical prowess of a standard quantum chemical package such as GAUSSIAN '98 [26] to employ a density functional theory (DFT)-based method for evaluating an F matrix. The F matrix is then supplemented with self-energy matrices $\Sigma_{1,2}$ describing an open system connected to the two contacts and involving the detailed contact microstructure, while the nonequilibrium (transport) part is set up using the nonequilibrium Green's function (NEGF) formalism [27]. We refer the reader to our past work for details of the NEGF equations and the calculation of the self-energy matrices [28,29,17]. In this article, we will concentrate mainly on the physical insights.

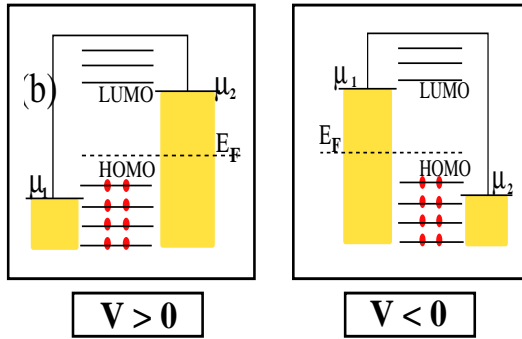


FIG. 2. Onset of conduction is given by the voltage where either of the contact chemical potentials $\mu_{1,2}$ crosses the nearest conducting molecular level, HOMO in this case.

The coupled DFT-NEGF formulation of molecular electronics is in effect the generalization of the coupled

Poisson-hydrodynamic equations used extensively in analyzing device transport [30,31]. We supplement the Poisson (Hartree) term with exchange-correlation corrections that are small in macroscopic devices but significant in molecules, while the semiclassical hydrodynamic equation is replaced with a fully quantum mechanical NEGF formalism [32].

The self-consistent formalism described above is completely general, and can be employed in modeling transport through a wide variety of physically different systems. For instance, we have used this scheme to obtain semi-empirical [3,33] and first-principles density functional (DFT)-based (LANL2DZ/B3PW91) [17,36] I-V characteristics of metallic quantum point contacts as well as semi-conducting aromatic thiol molecules bonded to Au(111) surfaces. Whether one is dealing with a carbon nanotube, a ballistic MOSFET [33,34], a spin transistor, a resonant tunneling diode [35] or a molecular wire, the above formalism holds. One needs simply to evaluate each of the following quantities: (i) an appropriate Fock matrix F describing the device; (ii) a contact Fermi energy E_F relative to which the device levels are evaluated and which determines the electrochemical potentials $\mu_{1,2}$; (iii) a self-consistent potential U_{SCF} describing charging effects and the electrostatic influence of the environment (this term is incorporated into the effective F matrix of the device), and (iv) a set of self-energy matrices $\Sigma_{1,2}$ that describe the coupling of the device with the contact, the matrices depending on the contact surface Green's function as well as the device-contact bonding geometry. Additional self-energy matrices can be introduced to describe scattering, by phonons or polarons for example. Within the same self-consistency scheme and NEGF prescription, one can then get qualitatively different I-V characteristics just by varying F , E_F , U_{SCF} and

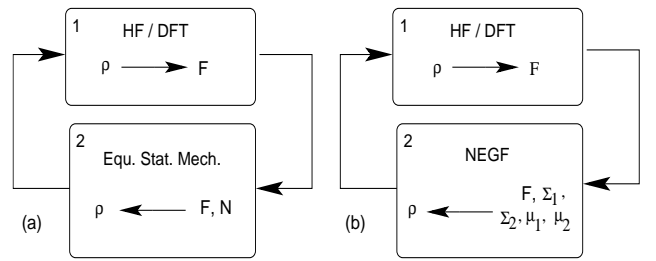


FIG. 3. Self-consistency schemes: (a) for an isolated molecule in equilibrium, one calculates the Fock matrix F starting with a guess density matrix ρ , and fills up the corresponding levels with N electrons to get back ρ ; (b) for an open system, the molecular Fock matrix is supplemented with self-energy matrices $\Sigma_{1,2}$ describing coupling with the contacts. An applied bias drives the system out of equilibrium due to two different contact chemical potentials $\mu_{1,2}$. The step from F to ρ is different from (a), and is obtained by solving the NEGF equations [32].

The effect of each of the above parameters on the molecular I-V is schematically shown in Fig. 1. The conductance gap depends on $(E_F - E_{MOL})$, and the maximum current level is set by the parallel combination $\Gamma = \Gamma_1 + \Gamma_2 = \Gamma_1 \Gamma_2 / (\Gamma_1 + \Gamma_2)$ of the individual contact broadenings $\Gamma_{1,2} = \Gamma_0 (1 + \frac{U_0}{E_F - E_{MOL}})$. The current rises over a width which depends on the total broadening of the molecular levels, which in turn depends on (a) the thermal broadening $k_B T$, (b) the series combination $\Gamma = \Gamma_1 + \Gamma_2$ of the contact broadenings $\Gamma_{1,2}$ and (c) the Coulomb charging energy U_0 to add an extra charge to the molecule (the charging energy tends to drag out the conductance peak, so that for appreciable charging energies, the contact chemical potentials may not be able to cross a molecular level easily under bias, resulting in a relatively featureless I-V characteristic). Finally, the potential profile across the molecule sets the overall voltage division factor β which determines the prefactor in the ratio between the conductance gap and $E_F - E_{MOL}$ ($\beta = 0.5$ and the prefactor equals 4 for symmetric coupling, as in Fig. 1). The voltage division factor β depends on the contact geometries and characterizes the Laplace part of the potential, while the Poisson part describes self-consistent charging effects, and is characterized by U_0 .

We summarize below the most challenging and physically relevant questions in obtaining a molecular I-V characteristic:

Where is the contact Fermi energy relative to the molecular levels? ($E_F; E_{MOL}$)

What is the broadening due to the contacts? ($\Gamma_{1,2}$)

What is the spatial profile of the Laplace potential? (β)

What is the charging energy? (U_0)

Note that each of the above quantities is in general a complicated matrix that can be modeled independently using either semi-empirical or first-principles methods. However, in order to develop a "feel" for how these quantities affect the molecular I-V as in Fig. 1, we will try to capture their essence in terms of a few characteristic scalar parameters, as defined above. We will now address the influence of each parameter one at a time below.

II. MOLECULAR CONDUCTION: HOW CAN WE MODEL IT?

A. Where is the contact Fermi energy relative to the molecular levels?

This is probably the most challenging problem to sort out. One needs to start by modeling the quantum chemistry of the molecule. For our candidate molecule phenyl

dithiol (PDT), shown in Fig. 4, it is believed that the sulphur atoms bond with a Au(111) surface by desorption of the end hydrogen atoms that are then replaced by a triangle of gold atoms with sulphur sitting above their centroid [37]. The energy levels of the isolated PDT molecule compare well with those obtained by replacing each H-atom by three gold atoms (the gold atoms introduce some additional localized levels in the HLG). Replacing the gold cluster with a self-energy describing metallic gold broadens the molecular levels into a quasi-continuous spectrum, with the localized levels developing into metal-induced gap states (MIGS) decaying spatially away from the contacts into the molecular center. Now, the energy levels of the isolated molecule itself depend sensitively on the method of calculation (a comparison plot is shown in Fig. 4). Different theoretical groups have adopted different first-principles schemes in their analysis [17,20], so the unanswered question at this point is: which method is appropriate for calculating the single-particle energy levels of an open subsystem under bias?

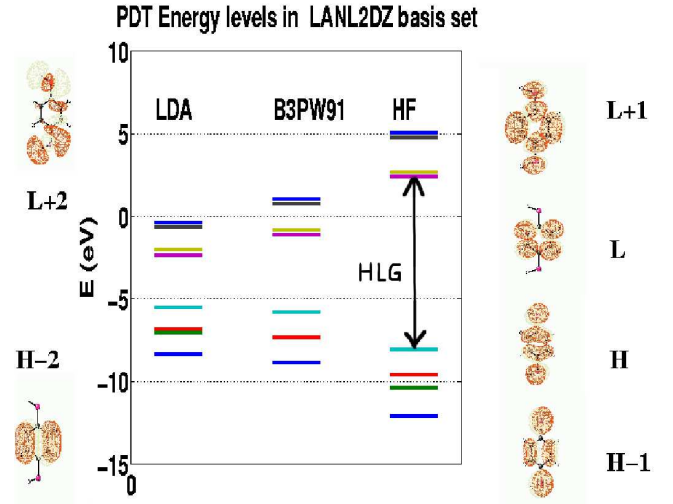


FIG. 4. The single-particle molecular energy levels of PDT vary considerably for density functional-based and Hartree-Fock methods, giving different conductance gaps. The orbital wave functions agree for all the different methods and for various choices of basis sets (symbols H: HOMO, L: LUMO, HLG: HOMO-LUMO gap, LDA: Local Density Approximation, B3PW91: 3 parameter Becke exchange and Perdew-Wang 91 correlation, HF: Hartree-Fock).

What is consistent among the various methods of calculation, including semi-empirical (Huckel-based) theories, is the overall shape of the orbital wave functions; for instance, the HOMO is largely sulphur-based and delocalized while the LUMO is ring-based and localized. This would seem to suggest a broad HOMO DOS and a sharp LUMO DOS, although theories don't seem to agree even on this point (see for example Fig. 22 in [28]).

and Fig. 3 in [38]). The difference could arise due to different bonding geometries assumed at the gold-thiol interface. Thus the intrinsic chemistry of the molecular system needs to be cleared up, and theoretical agreement reached on the equilibrium molecular bonding properties before the transport-related issues can be sorted out.

The position of the contact Fermi energy E_F relative to the molecular energy levels is also an unsettled issue. The Fermi energy depends sensitively on the specimen model for the contact geometry. Different models for the contact (for instance DFT-based [20,17], Bethe lattice [21], jellium [19]) can give different charge contents and level broadenings of the molecule, as well as different work functions for the bulk electrodes. This could cause an appreciable shift in E_F , given the rather small gap density of states in the molecular HLG. Given that for extensively studied systems such as metal-semiconductor interfaces the precise location of E_F is still an active topic of research [39], perhaps the best one can do at this point is to inquire if E_F is closer to the molecular HOMO or LUMO level, the analogous question for a semiconductor being whether it is p-type or n-type.

Conceptually the cleanest way to address the equilibrium Fermi energy problem is by including a few layers of the contact as a cluster in a "supermolecule", which would act as the device under investigation. Hereafter the contact is assumed unaltered during conduction, with all the "action" lying in the device sector. The advantages of including such a cluster are enormous (for a discussion, see [36]), such as the automatic inclusion of image charges (the supermolecule is charge neutral), avoiding uniqueness issues related to partitioning in a non-orthogonal, non-localized, atomic basis set and the proper treatment of the surface physics. Ideally, the cluster size should be significantly larger than the atomic Debye length of the contact material, while for practical purposes, it is usually limited by computational resources. E_F is usually set by the HOMO of the (large) supermolecule, while the molecular levels can be identified by either plotting the wavefunctions or by computing the local density of states (LDOS) on the molecule. To employ this scheme to sort out the molecular chemistry and energy level structure, it is essential that the contact cluster and the molecule be calculated using the same scheme (DFT/tight-binding, etc). Attempts at performing such a computation at the semi-empirical [10] and DFT [40] levels have yielded a Fermi energy quite close to the HOMO level for PDT-Au(111) heterostructures.

The experimental situation is somewhat unclear. The conductance gap for PDT itself is different for different experimental geometries. The gap is around 3 volts for break junction measurements by Reed et al. [1] and around 4 volts for STM measurements by Hong et al. [41], while corresponding break junction measurements by David Janes' group at Purdue indicate featureless I-V characteristics with no discernible conductance gap [42].

Since the gap depends on E_F which is likely to be different for the two experimental contact geometries, and could further be compromised by the presence of charging in the system, such a difference is not surprising. It is also not clear whether the conduction is through a single molecule bridging the junctions, or a series combination of molecules attached separately to the two junctions [43]. It seems sensible therefore to treat E_F as a fitting parameter, in the absence of precise characterization of the contact surfaces and molecular geometry. Alternatively, one could dictate the position of E_F relative to the levels, guided by separate equilibrium cluster calculations, as discussed earlier.

Experiments incorporating a third terminal (gate) can help clarify some of these issues appreciably. For instance, a positive gate voltage lowers the molecular levels so that the Fermi energy approaches the LUMO and moves away from the HOMO. For a purely electrostatic gate control mechanism, a measured decrease in conductance will suggest HOMO (p-type) conduction, while the reverse result indicates LUMO (n-type) conduction.

Summary: Need to model the molecule and the contact bonding self-consistently within the same scheme, doing justice to the molecular quantum chemistry as well as the contact surface microstructure. The method of calculating the energy levels or the Fermi energy is still an unresolved issue.

B. What is the broadening due to the contacts?

Although experimental knowledge of the contact conditions is difficult to access, could one at least hope to model a particular idealized contact geometry and obtain an appropriate self-energy? We obtain the self-energy matrices $\Sigma_{1,2}$ formally by an exact partitioning of the infinite metal molecule-metal system, projecting its single particle Green's function onto the device subspace [36].

$\Sigma_{1,2}$ depend on the contact surface Green's function and the contact-molecular bondings. We obtain the couplings at the surface by simulating a large cluster from the contact coupled to the device and calculating its overlap and Fock matrices. The contact surface Green's function is calculated using a recursive Green's function technique taking the full group theory of the FCC Au(111) crystal surface into account [11,17].

One can replace the partitioning scheme with a scattering-formalism [19,12,10,13] that deals with the entire infinite system. Ideally, both methods (scattering formalism and the NEGF prescription) should yield the same answer; however, there is a conceptual simplification in partitioning the problem into a "device" part involving the electronically active molecule, and a "contact" part determining the lead-molecular interactions. These involve two entirely different areas of research,

quantum chemistry and surface physics, so partitioning allows us to improve modeling each of them independently. Moreover, NEGF naturally allows us to include incoherent processes, which can be important even for a short molecule if there are localized states that cannot be populated from the contacts [28,36].

How do we know if we have modeled our contacts correctly? The overall "shape" of the molecular I-V can be obtained approximately without getting the bonding or the quantum chemistry right. One excellent benchmark is the quantum point contact (QPC) [23], the I-V characteristic of which is experimentally measured to be ohmic, with a conductance quantized in units of $G_0 = 2e^2/h \approx 77.5$ S [44]. Starting with a six atom gold chain coupled to Au(111) contacts describing a QPC, we get a conductance quantized ohmic I-V, as expected [17,36]. This is highly nontrivial, because conductance quantization arises out of a molecule that is perfectly transmitting over a band of energies between ϵ_1 and ϵ_2 (aside from Fabry-Pérot type oscillations). This requires the self-energy matrices to couple the wire with the contacts seamlessly without introducing any spurious reflections. To illustrate the sensitivity of the quantization on the coupling, we scaled the overall matrix elements by a factor of ν ; the resultant I-V ceases to be ohmic, and resembles that of a resonantly conducting system such as PDT (Fig. 5 (i)).

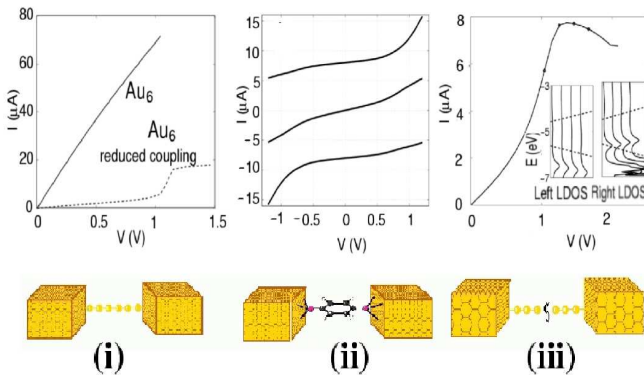


FIG. 5. Calculated two-terminal I-V characteristics for different molecular geometries: (i) ohmic I-V with a quantized conductance (adapted from [17]) for a quantum point contact (QPC) consisting of a six-atom gold chain connected to Au(111) contacts; (ii) a symmetric, resonant I-V for PDT that turns asymmetric (upper and lower curves) (adapted from [57]) on altering the relative coupling strengths to the contacts; (iii) negative differential resistance (NDR) in the I-V for a QPC with a barrier in the middle (adapted from [36]).

The above exercise is a good check of the accuracy of the contact broadenings. Once the surface Green's functions are deemed to be correct, it is an easy matter to replace the Au_6 molecular cluster with the molecule of choice and proceed with calculating its I-V.

Summary: The QPC can be used as a benchmark for testing out the self-energy matrices. The couplings at the surface and the contact surface Green's functions need to be calculated accurately, including the overall group theory of the metal crystal comprising the leads.

C. What is the spatial profile of the Laplace potential?

The electrostatic potential profile across the molecule can be separated into two parts: (i) the Laplace part describes the influence of the contact geometries in the absence of charges and screening effects; (ii) the Poisson part involves screening by the charges, and is determined by the charging energy of the molecule. In this section, we will concentrate on the Laplace part, and address the charging-related issues associated with the Poisson part in the next section.

The Laplace part of the potential profile is set by the relative capacitances of the contacts, and can be determined rigorously by solving the 3-D Laplace equation with the correct potential boundary conditions for the contacts. The Laplace part is characterized by the voltage-division factor β which describes the proportion in which the applied voltage drops across the various contact-molecular interfaces. A convenient way to analyze the potential profile across the molecule is to incorporate the voltage-division factors in the definitions of the contact electrochemical potentials $\mu_{1,2}$, which would keep the molecular levels themselves fixed under drain bias in the absence of charging (next section) and move them under gate bias alone. For a two-terminal device appreciable current flow requires the capacitive couplings with the source and drain electrodes to be roughly equal (although their resistive (quantum) couplings $\gamma_{1,2}$ could still be quite different), leading usually to $\beta \approx 0.5$.

Although the Laplace part involves essentially nineteenth century classical electrostatics, it can substantially influence device I-V characteristics. In a gated three-terminal device, for instance, a good gate control mechanism in a well-designed ballistic conductor essentially involves trying to keep the charge density near the source end of the conductor constant by pinning the device DOS to the source chemical potential [51]. This gives an effective $\beta = 1$, so that as the drain chemical potential ventures into the HLG under bias, the current starts to saturate [52]. Note that this saturation mechanism is entirely different from saturation in two-terminal molecular devices, which occurs when either contact chemical potential has just crossed a molecular level and another level has not yet kicked in. In contrast to the two-terminal I-V, the three-terminal characteristic is asymmetric with respect to source-drain bias. Since the gate determines the position of the equilibrium Fermi energy through the

Laplace solution, it leads to gate-modulation of the ON current in such devices.

A gate can influence the molecular electronic properties in a variety of ways: it could have a purely electrostatic effect on the channel charge and correspondingly the molecular levels, as described above. However, as pointed out by Damle et al. [52], good electrostatic gate control is not possible for a 10 Å molecule such as PdT, unless the gate oxide is prohibitively thin. Additionally, the gate can alter the properties of the contact-molecular interfaces (Schottky-barrier type effects [53]), or even alter the conformations of the active molecule [54], all of which could affect the shape of the molecular I-V.

Another example where the Laplace solution itself can influence the molecular I-V characteristic involves conduction mechanisms that require the alignment/misalignment of energy levels localized on different parts of the molecule. For instance, the Aviram-Ratner mechanism [49] involves a donor-bridge-acceptor system where the Laplace part of the self-consistent potential aligns the levels at the two ends for positive bias, and misaligns them for negative bias, leading to a strongly rectifying I-V characteristic. A similar example involves a quantum point contact (QPC) with a stretched bond in the middle (Fig. 5(iii)). The defect disconnects the LDOS on its two sides, allowing them to separately equilibrate with the two contacts and follow their respective chemical potentials under source-drain bias. Within the window set by μ_1 and μ_2 , the Laplace solution causes the LDOS on the two sides to slide past each other (figure inset). Since this amounts to two transmission peaks sliding in and out of resonance, the resulting I-V shows a weak negative differential resistance [36,50].

Summary: The Laplace part of the 3-D electrostatic potential profile needs to be calculated using the boundary conditions set by the electrodes. The Laplace potential can significantly affect the molecular I-V characteristic, by aligning or misaligning different parts of the molecular LDOS or by pinning the molecular DOS to one of the electrodes in the presence of a gate terminal.

D. What is the charging energy?

The Poisson part of the potential profile carries information about screening and charging inside the molecule, and is characterized by $U_0 D_0 = C_Q = C$, where $U_0 = e^2/C$ is the Coulomb charging energy, D_0 is the molecular gap DOS, the quantum capacitance $C_Q = e^2 D_0$, and C describes the total electrostatic capacitive coupling to the various electrodes. The charging energy U_0 describes the "ease" with which the molecular levels can be filled or emptied, and tends to drag out the I-V characteristic as shown in Fig. 1. Note that the effect of charging can be looked upon as a voltage-dependent

(V). The net capacitance C contributing to U_0 is determined by the geometry and dielectric constant of the molecule and the electrodes. For instance, while 10 Å InAs spherical quantum dots have low charging energies

100 meV [55], a 10 Å isolated PdT molecular wire has a much larger charging energy $\sim 3-4$ eV, making it a lot harder to cross a level with a drain bias. At even higher charging energies $U_0 \sim 1/2$, one can get many-body effects such as Coulomb Blockade and Kondo resonance. While some Coulomb-Blockade type effects can be captured within an effective one-particle self-consistent field model within an unrestricted calculation [29] (such as unrestricted Hartree-Fock or spin density functional theory), doing justice to these problems requires us to go beyond the one-particle prescription we have used so far.

The Poisson solution describes the effect of adding or removing charge from the molecule, as well as the effect of redistribution of charge within the molecule, responsible for screening of the applied voltage. The efficiency of the screening process depends on the amount of material available for the reorganization of the charges. For a molecular wire much thinner than the Debye length, the net electrostatic potential is essentially given by the Laplace solution of the previous section, leading to a ramp-like potential profile [17,36,45,47]. In contrast, a thick metallic wire allows sufficient screening, yielding a potential profile that is essentially flat [36,45,46]. Such a flat potential profile can be obtained even with a thin molecular wire if the latter is embedded in a dielectric medium as part of a self-assembled monolayer (SAM), in which case the neighboring wires screen the potential profile. One way to model a SAM would be to disallow any transverse variations in charge or electrostatic potential, which would amount in effect to solving the 1-D Poisson equation. This would give a highly screened potential profile even with a thin molecular wire [48,45].

Charging can lead to very interesting effects, such as the creation of an asymmetric I-V with a spatially symmetric molecule [5,56]. Consider a symmetric molecule with unequal resistive (quantum) couplings to the two contacts ($\Gamma_1 \neq \Gamma_2$). Near the onset of current conduction through a HOMO level, a negative bias on the strong contact keeps it filled, while a positive bias empties it. Since the molecule gets positively charged one way but not the other, the I-V is dragged out asymmetrically such that one gets a lower current for positive bias on the stronger contact. Interestingly for conduction through a LUMO level, the sense of the I-V asymmetry reverses [57], because one now needs to fill the LUMO to charge up the molecule. This allows us to identify the nature of the conducting molecular orbital, which is important given that different orbitals conduct quite differently. For PdT, STM data [3] (the STM tip being the weaker contact) seems to indicate HOMO-based conduction. Our results (Fig. 5(ii)) qualitatively match the I-V characteristics obtained by Reichert et al. [5], with an initially

symmetric I-V that turns weakly asymmetric on drawing either contact away from the molecule.

The total electrostatic potential profile is the sum of the Laplace and Poisson parts, which have different effects on the molecular I-V. For typical break-junction/STM measurements on molecules such as PDT, $C_0 = C = U_0 D_0 \ll 1$, and the overall potential profile is essentially given by the Laplace potential with the net voltage dividing up as the capacitance ratio between the electrodes. If however the molecule is so strongly coupled to the substrate that there are appreciable MIGS, D_0 becomes large enough that $C_0 = C$ starts to become important. In the limit of $C_0 = C \gg 1$, the I-V gets dragged out substantially by charging (Fig. 1), and the natural self-consistent voltage divides between the source and drain contacts according to their resistance ratio $\alpha_2 = (\alpha_1 + \alpha_2)$. This situation arises for metal nanoclusters probed by an STM tip. Since the resistance is much larger at the STM end, much of the applied voltage drops across the STM-cluster gap, so that the cluster levels remain pinned to the substrate, and the STM chemical potential alternately scans the HOMO and LUMO levels under opposite drain bias.

Summary: The charging energy can turn an otherwise symmetric I-V into an asymmetric one. Given a spatially symmetric molecule, we predict a larger current for positive bias on the stronger contact and HOMO conduction, while for LUMO conduction, the sense of the I-V asymmetry is reversed.

III. COMPUTATIONAL ISSUES

A brief discussion of computational issues is perhaps in order. The calculation of molecular conductance requires two steps, (a) calculating a Fock matrix given a density matrix, and (b) calculating a density matrix from the Fock matrix. The first step is the most computationally challenging part, involving the evaluation of DFT-based exchange-correlation integrals which are quite numerically complicated, especially in sophisticated basis sets involving relativistic core pseudopotentials. We find our own LDA calculation of the molecular Fock matrix in a minimal basis set to be comparable in accuracy, but not in speed, with GAUSSIAN 98. Therefore we let GAUSSIAN 98 do this part, exploiting decades of development that have gone into it. The second step requires contact self-energy matrices which can be calculated once and for all for realistic contact surface structures (e.g., Au(111) contacts) using a real space recursive Green's function technique. The contact coupling matrices can be simulated in GAUSSIAN 98 with a finite-sized cluster, with care exercised to eliminate edge effects on the structure of the contact surface Green's function [36] (a suitable localized basis describing gold would sort out this problem

automatically).

The computational challenge for us is to solve the NEGF equations, requiring us to find the number of electrons on the molecule. Such a requirement amounts to integrating the nonequilibrium electron DOS all the way from the bottom of the contact band to the Fermi energy. Since the Green's functions entering the DOS expression are highly peaked around the molecular levels, this process involves integrating over an energy range of several hundred volts with a millivolt accuracy for each bias point and each step of the self-consistent procedure. We have addressed this problem in two ways: (i) assuming a weak (in practice, constant) energy-dependence of the self-energy matrices (valid for Au(111) which has an energy-independent DOS near E_F), one can then perform the integrals analytically [36]; (ii) the nonequilibrium DOS can be divided into two groups, one lying outside the domain of $\alpha_{1,2}$, and the rest inside that window. The first part can be integrated using a contour integration scheme [20], while the part between $\alpha_{1,2}$ can be calculated either by brute force grid-based integration over the finite range between α_1 and α_2 , or by reverting to the constant approximation. Although our calculations are performed with LANL2DZ basis sets which are somewhat delocalized, it is preferable to employ relatively localized basis sets in order to avoid issues related to partitioning and to be consistent with the tight-binding approach that we are using here [23]. Different approximations give different values of the total electron count, thereby affecting the equilibrium Fermi energy position, which clearly needs more attention. However, the approximations allow us to obtain first-principles DFT-based I-Vs for a molecule like PDT in a few hours on a SUN workstation, taking into account the details of the contact geometry.

IV. ISSUES WE HAVEN'T COVERED

We have seen that by appropriately modeling each experimental geometry, we can get qualitatively and quantitatively different conductance properties, ranging from ohmic to rectifying, switching and saturating I-V characteristics. We now outline three of the issues that we have ignored so far, namely, Conformation, Incoherence and Correlation.

(i) Conformation. One of the principal advantages of a molecule is that it is semi-rigid. This means that the conformation of a molecule can be altered, by transferring charge or applying an external field. Encouraging experimental indications of a conformationally mediated I-V have been obtained, for a fullerene-based transistor [58], and for the redox sidegroup-specific [2] or vibrationally mediated [59] NDR measurements. We are currently investigating the role of conformational changes, in conjunction with charging and gate electrostatics, in

modulating the molecular I-V [54] in a three-term inelastic-vice.

(ii) Incoherence. For long molecules, molecular vibrations are important as sources of incoherent or inelastic scattering, leading to hopping or polaronic transport (see for e.g. [60]). Such inelastic effects can be naturally included in the NEGF formalism, requiring us to introduce another self-energy matrix describing the connection of the molecule with the source of the inelastic scattering (a phonon bath, for example) [36,45,61]. In the tunneling regime, in particular, inelastic scattering turns out to be crucial for transport and dissipation in long molecular wires, such as DNA.

(iii) Correlation. Finally, there are examples of molecular measurements such as the Kondo effect [62], where the physics of current flow cannot be captured in terms of a simple one-particle picture, and require the incorporation of many-body correlation effects in our model. We leave these problems for future work.

We would like to thank P. Damle, D. Janes, A. Liang, S. Lodha, M. Lundstrom, M. Paulsson, T. Rakshit, R. Reifengerger, R. Venugopal and F. Zahid for useful discussions. This work has been supported by the US Army Research Office (ARO) under grant number DAAD19-99-1-0198.

[1] M. A. Reed, C. Zhou, C. J. Muller, T. P. Burgin and J. M. Tour, *Science* 278, 252 (1997).
 [2] J. Chen, M. A. Reed, A. M. Rawlett and J. M. Tour, *Science* 286, 1550 (1999).
 [3] W. Tian, S. Datta, S. Hong, R. Reifenberger, J. I. Henderson and C. P. Kubiak, *J. Chem. Phys.* 109, 2874 (1998).
 [4] C. P. Collier, E. W. Wong, M. Belohradsky, F. M. Raymond, J. F. Stoddart, P. J. Kuekes, R. S. Williams, J. R. Heath, *Science* 285, 391 (1999).
 [5] J. Reichert, R. Ochs, D. Beckmann, H. B. Weber, M. Mayor and H. v. Lohneysen, *Phys. Rev. Lett.* 88, 176804 (2002).
 [6] A. Dhirani, P.-H. Lin, P. Guyot-Sionnest, R. W. Zehner and L. R. Sita, *J. Chem. Phys.* 106, 5249 (1997).
 [7] X. D. Cui, A. Primak, X. Zarate, J. Tomfohr, O. F. Sankey, A. L. Moore, T. A. Moore, D. Gust, G. Harris and S. M. Lindsay, *Science* 294, 571 (2001).
 [8] D. Porath, A. Bezryadin, S. de Vries and C. Dekker, *Nature* 403, 635 (2000).
 [9] B. Chen and J. M. Metzger *J. Phys. Chem. B* 103, 4447 (1999).
 [10] E. G. Emberly and G. Kirczenow, *Phys. Rev. B* 58, 10911 (1998).
 [11] M. Samanta, Master's thesis, Purdue University, 1999.
 [12] M. Paulsson and S. Stafstrom, *Phys. Rev. B* 64, 035416 (2001).

[13] P. Sautet and C. Joachim, *Phys. Rev. B* 38, 12238 (1988).
 [14] L. E. Hall, J. R. Reiners, N. S. Hush and K. Silverbrook, *J. Chem. Phys.* 112, 1510 (2000).
 [15] S. N. Yaliraki and M. A. Ratner, *J. Chem. Phys.* 109, 5036 (1998).
 [16] G. Cuniberti, G. Fagas and K. Richter, *Chem. Phys.* 281, 465 (2002).
 [17] P. S. Damle, A. W. Ghosh and S. Datta, *Phys. Rev. B Rapid Commun.* 64, 201403 R (2001).
 [18] P. A. Derosa and J. M. Seminario, *J. Phys. Chem. B* 105, 471 (2001).
 [19] M. Di Ventura, S. T. Pantelides and N. D. Lang, *Phys. Rev. Lett.* 84, 979 (2000).
 [20] J. Taylor, H. Guo and J. Wang, *Phys. Rev. B* 63, 245407 (2001).
 [21] J. J. Palacios, A. J. Perez-Jimenez, E. Louis and J. A. Verges, *Phys. Rev. B* 64, 115411 (2001).
 [22] J. J. Palacios, A. J. Perez-Jimenez, E. Louis E. San-Fabian and J. A. Verges, *Phys. Rev. B* 66, 035322 (2002).
 [23] M. Brandbyge, J.-L. Mozos, P. Ordejon, J. Taylor and K. Stokbro, *Phys. Rev. B* 65, 165401 (2002).
 [24] A. W. Ghosh, F. Zahid, S. Datta and R. R. Birge, *Chem. Phys.* 281, 225 (2002), Special issue on Processes in Molecular Wires, ed. P. Hanggi, M. Ratner and S. Yaliraki.
 [25] R. H. Herman, *J. Chem. Phys.* 39, 1937 (1963).
 [26] H. B. Schlegel et al., *Gaussian 98*, Revision A.7. Gaussian, Inc., Pittsburgh PA, 1998.
 [27] A similar prescription has been used for the equilibrium problem by Xue et al. (see Y. Xue, Ph.D. Thesis, Purdue University (2000)).
 [28] F. Zahid, M. Paulsson and S. Datta, to appear in forthcoming volume on Advanced Semiconductor and Organic Nano Techniques, ed. H. Morkoc, Academic Press. Also described on Huckel-IV 2.0 on the nanoHUB, <http://www.nanohub.purdue.edu>.
 [29] M. Paulsson, F. Zahid and S. Datta, in "Nanoscience, Engineering and Technology Handbook", edited by W. Goddard, D. Brenner, S. Lyshevski and G. Iafrate, CRC Press.
 [30] H. U. Baranger and J. W. Wilkins, *Phys. Rev. B* 30, 7349 (1984).
 [31] S. Selberherr, "Analysis and Simulation of Semiconductor Devices" Springer-Verlag, New York 1984.
 [32] S. Datta, "Electronic Transport in Mesoscopic Systems", Cambridge University Press (1995).
 [33] P. S. Damle, A. W. Ghosh and S. Datta, Book chapter in *Molecular Electronics*, ed. Mark A. Reed, in press.
 [34] R. Venugopal, Z. Ren, M. S. Lundstrom and D. Jovanovic, *J. Appl. Phys.* 92, 3730 (2002).
 [35] R. Lake and S. Datta, *Phys. Rev. B* 45, 6670 (1992).
 [36] P. S. Damle, A. W. Ghosh and S. Datta, *Chem. Phys.* 281, 171 (2002), Special issue on Processes in Molecular Wires, ed. P. Hanggi, M. Ratner and S. Yaliraki.
 [37] The centroid geometry is suggested by model calculations: see for example, N. B. Larsen, H. Biebuyck, E. Delamarche and B. Michel, *J. Am. Chem. Soc.* 119, 3107 (1997); N. Camillone, C. E. D. Chidsey, G. Y. Liu and G. Scoles, *J. Phys. Chem.* 98, 3503 (1993). Based on this, we adopt this model geometry for our specific contact-molecular bonding scheme, although there are theoretical

suggestions and experimental indications otherwise.

- [38] M. Di Ventura, S. T. Pantelides and N. D. Lang, Appl. Phys. Lett. 76, 3448 (2000).
- [39] See for example W. E. Spicer and A. M. Green, J. Vac. Sci. Technol. B 11, 1347 (1993); R. T. Tung, J. Vac. Sci. Technol. B 11, 1546 (1993); R. T. Tung, Mat. Sci. Eng. Rep. 35, 1 (2001).
- [40] H. B. Weber, J. Reichert, F. Weigand, R. Ochs, D. Beckmann, M. Mayor, R. Ahlrichs and H. v. Lohneysen, Chem. Phys. 281, 113 (2002), Special issue on Processes in Molecular Wires, ed. P. Hanggi, M. Ratner and S. Yaliraki.
- [41] S. Hong, R. Reifemberger, W. Tian, S. Datta, J. Henderson and C. P. Kubiak, Superlattices and Microstructures 28, 289 (2000).
- [42] D. Janes, private communications.
- [43] E. G. Emberly and G. Kirczenow, Phys. Rev. B 64, 235412 (2001).
- [44] H. Ohnishi, Y. Kondo and K. Takayanagi, Nature (London) 395, 780 (1998).
- [45] A. Liang, A. W. Ghosh and S. Datta, in preparation.
- [46] A. Nitzan, M. Galperin, G. Ingold and H. Grabert, cond-mat/0207124; A. Nitzan, M. Galperin, G. Ingold and H. Grabert, cond-mat/0209091.
- [47] N. Lang and P. Avoiris, Phys. Rev. Lett. 84, 358 (2000).
- [48] V. Mujica, A. Roitberg and M. Ratner, J. Chem. Phys. 112, 6834 (2000).
- [49] A. Aviram and M. A. Ratner, Chem. Phys. Lett. 29, 274 (1974).
- [50] M. Paulsson, Ph.D. thesis, Linköping University, 2000.
- [51] M. Lundström and Z. Ren, IEEE Trans. Electron Devices 49, 133 (2002).
- [52] P. Damle, T. Rakshit, M. Paulsson and S. Datta, cond-mat/0206328.
- [53] M. P. Leppel and S. M. Sze, Proc. IEEE 56, 1400 (1968); J. R. Rucker, C. Wang and P. Scott-Camey, Appl. Phys. Lett. 65, 618 (1994).
- [54] A. W. Ghosh, T. Rakshit and S. Datta, cond-mat/0212166.
- [55] U. Banin, Y. Cao, D. Katz and O. Mello, Nature 400, 542 (1995).
- [56] C. Kergueris, J.-P. Bourgois, S. Palacin, D. Esteve, C. Urbina, M. Magoga and C. Joachim, Phys. Rev. B 59, 12505 (1999).
- [57] A. W. Ghosh, F. Zahid, P. S. Damle and S. Datta, cond-mat/0202519.
- [58] H. Park, J. Park, A. K. L. Kim, E. H. Anderson, A. P. Alivisatos and P. L. McEuen, Nature 407, 57 (2000).
- [59] J. Gaudioso, L. J. Lauhon and W. Ho, Phys. Rev. Lett. 85, 1918 (2000).
- [60] H. Ness and A. J. Fisher, Phys. Rev. Lett. 83, 452 (1999).
- [61] X.-Q. Li and Y. Yan, Appl. Phys. Lett. 79, 2190 (2001).
- [62] J. Park, A. N. Pasupathy, J. I. Goldsmith, C. Chang, Y. Yaish, J. R. Petta, M. Rinkoski, J. P. Sethna, H. D. Abruna, P. L. McEuen and D. C. Ralph, Nature 417, 722 (2002); W. J. Liang, M. P. Shores, M. Bockrath, J. R. Long and H. Park, *ibid*, 725 (2002).